Journal of Computational Mathematics
Vol.xx, No.x, 2023, 1–24.

http://www.global-sci.org/jcm
doi:10.4208/jcm.2305-m2022-0171

A UNIFORM CONVERGENT PETROV-GALERKIN METHOD FOR A CLASS OF TURNING POINT PROBLEMS*

Li Feng
Department of Mathematical Sciences, Tsinghua University, Beijing 100084, China
Email: feng-l18@mails.tsinghua.edu.cn
Zhongyi Huang[1)]
Department of Mathematical Sciences, Tsinghua University, Beijing 100084, China
Email: zhongyih@mail.tsinghua.edu.cn

Abstract

In this paper, we propose a numerical method for turning point problems in one dimension based on Petrov-Galerkin finite element method (PGFEM). We first give a priori estimate for the turning point problem with a single boundary turning point. Then we use PGFEM to solve it, where test functions are the solutions to piecewise approximate dual problems. We prove that our method has a first-order convergence rate in both L_h^∞ norm and a discrete energy norm when we select the exact solutions to dual problems as test functions. Numerical results show that our scheme is efficient for turning point problems with different types of singularities, and the convergency coincides with our theoretical results.

Mathematics subject classification: 65N06, 65B99.
Key words: Turning point problem, Petrov-Galerkin finite element method, Uniform convergency.

1. Introduction

Singularly perturbed problems have been widely studied in the fields of fluid mechanics, aerodynamics, convection-diffusion process, etc. In such problems, there exist boundary layers or interior layers because a small parameter is included in the coefficient of the highest derivative. Consider the following singularly perturbed turning point problem in one dimension:

$$\begin{cases} Lu = -\varepsilon u'' + p(x)u' + b(x)u = f(x), \quad x_L < x < x_R, \\ u(x_L) = u_L, \quad u(x_R) = u_R, \end{cases} \tag{1.1}$$

where $p(x)$ has zeros $z_1 < z_2 < \cdots < z_m$ on $[x_L, x_R]$. We assume p, b, and f to be sufficiently smooth. Furthermore, we suppose

$$\begin{aligned} &b(x) - p'(x) \geq \gamma_0 > 0, \\ &b(x) \geq b_0 > 0 \end{aligned} \tag{1.2}$$

to ensure the well-posedness of the dual problems. Each zero of $p(x)$ is presumed to be a single root, i.e. $p'(z_i) \neq 0$.

From the asymptotic analysis, we know that there will be boundary/interior layers at some of z_i. Here we consider the following types of singularities:

* Received July 25, 2022 / Revised version received January 28, 2023 / Accepted May 26, 2023 / Published online November 2, 2023 /
[1)] Corresponding author

(a) Exponential boundary layers (singularly perturbed problems without turning points).

(b) Cusp-like interior layers (interior turning point problems).

(c) Boundary layers of other types (boundary turning point problems).

Singularly perturbed elliptic equations without turning points have been widely studied by researchers. Various numerical methods are utilized, where finite difference methods and finite element methods play prominent roles. El-Mistikawy and Werle [8] raise an exponential box scheme (EMW scheme) in order to solve Falkner-Skan equations. Kellogg *et al.* [2], Riordan and Stynes [28], etc., find this EMW scheme efficient when solving singularly perturbed elliptic equations. Fitted operator numerical methods, such as exponentially fitted finite difference method and Petrov-Galerkin method, are developed. Another class of methods, fitted mesh methods [6, 12, 16, 20, 31], show good adaptivity to different problems, while remeshing is necessary in some moving front problems.

A turning point problem is a class of equations in which the coefficient $p(x)$ vanishes at some points in the domain. Compared to singularly perturbed equations without turning points, interior layers and other types of boundary layers might appear in the solutions to turning point problems. O'Malley [24] and Abrahamson [1] analyze turning point problems in some common cases. Kellogg *et al.* [2] theoretically examine turning point problems with single interior turning points, and they use a modified EMW scheme, which obtains a first-order (or lower) convergence rate. Stynes and Riordan [28, 29] build a numerical scheme under Petrov-Galerkin framework and prove the uniform convergence in L^1 norm and L^∞ norm. Farrell [9] proposes sufficient conditions for an exponentially fitting difference scheme to be uniformly convergent for a turning point problem. Farrell and Gartland [10] modify the EMW scheme and construct a scheme with uniform first-order convergency, where parabolic cylinder functions are used in the computation. For other studies of turning point problems using fitted operator methods, please refer to [11, 21, 27, 34], for fitted mesh methods, please refer to [5, 19, 22, 25, 26, 30, 36].

We notice that most of the present research assume turning points to be away from the boundary. If a turning point meets an endpoint, the problem is called a boundary turning point problem, which has not been thoroughly studied. Vulanović [33] considers a turning point problem with an arbitrary single turning point and obtains uniform convergency using finite difference method on a non-equidistant mesh. Vulanović and Farrell [35] examine a multiple boundary turning point problem and make a priori estimates. However, estimates for single boundary turning point problems and numerical methods based on the uniform mesh are not given yet. In order to fill this blank, in this paper we estimate the derivatives of the solution to a standard single boundary turning point problem and raise an algorithm without particular mesh generation.

Petrov-Galerkin finite element method (PGFEM) is used in many problems. Dated back to 1979, Hemker and Groen [7] raise a method that treats problem (1.1) with Petrov-Galerkin method, where the coefficient $p(x)$ has a positive lower bound. The scheme in Farrell and Gartland [10] is based on the so-called patched function method, also interpreted as Petrov-Galerkin method. In references [3,4], Petrov-Galerkin method and discontinuous Petrov-Galerkin method are implemented in elliptic equations in two dimensions, demonstrating their efficiency and convergency.

Tailored finite point method (TFPM) is raised by Han *et al.* [15], which is designed to solve PDEs using properties of the solutions, especially for singularly perturbed problems. TFPM

could handle exponential singularities well, while simple difference methods might sometimes suffer from a low convergence rate. TFPM is later utilized in interface problems [17], steady-state reaction-diffusion equations [13], convection-diffusion-reaction equations [14], etc.

This study presents a numerical scheme to solve problem (1.1) with several types of singularities. We prove that the width of the boundary layer of a single boundary turning point problem is $\mathcal{O}(\sqrt{\varepsilon})$, which is a weaker version of the result in [35]. The derivative of the solution, u' is bounded by $C(1+\varepsilon^{-1/2})$ near the boundary layer and bounded by $C(1+x^{-1})$ away from the layer. We also prove the uniform convergence of the scheme in several discrete norms.

The rest of this paper is organized as follows. In Section 2, a priori estimates for continuous problems will be shown in each case. We use PGFEM to solve problem (1.1), where we choose (either exact or approximate) solutions to dual problems as test functions. We show details related to the numerical implementation in Section 3. Numerical results demonstrate the efficiency and the uniform first-order convergency of our scheme in Section 4. Finally, we give a brief conclusion in Section 5.

2. A Priori Estimates

In this section, we present a priori estimates for cases (a), (b), (c). First we briefly recall some results from previous work for cases (a) and (b). We will prove our estimates for case (c) later.

2.1. Exponential boundary layer

Suppose the velocity coefficient $p(x) \geq p_0 > 0$ (or otherwise, it has a negative upper bound). Eq. (1.1) is now written as

$$\begin{cases} Lu \equiv -\varepsilon u'' + p(x)u' + b(x)u = f(x), & -1 < x < 1, \\ u(-1) = u_L, \qquad u(1) = u_R, \\ p(x) \geq p_0 > 0, \quad b(x) \geq b_0 \geq 0. \end{cases} \tag{2.1}$$

The solution to (2.1) admits a boundary layer at $x = 1$ (at $x = -1$ if $p(x) \leq p_0 < 0$), and it is shown [2, 18] that the following estimates hold:

$$|u^{(k)}(x)| \leq C\left(1 + \varepsilon^{-k}\exp\left(-\frac{\eta(1-x)}{\varepsilon}\right)\right), \quad x \in (-1,1), \quad k = 0,1,2,\ldots, \tag{2.2}$$

where C, η are positive constants depending on u_L, u_R, f, p, b, which are independent of ε. We have the following property at once.

Proposition 2.1. *Suppose u is the solution to (2.1) and $p(x)$ is lower bounded, then there exists a constant C depending on u_L, u_R, f, p, b, which is independent of ε such that*

$$|(1-x)u'(x)| \leq C, \quad \forall x \in (-1,1). \tag{2.3}$$

2.2. Cusp-like interior layer

Suppose there is only one turning point $x = 0$, and Eq. (1.1) reads

$$\begin{cases} Lu \equiv -\varepsilon u'' + p(x)u' + b(x)u = f(x), & -1 < x < 1, \\ u(-1) = u_L, \quad u(1) = u_R, \\ p(0) = 0, \quad p'(0) < 0, \quad |p'(x)| \geq \dfrac{1}{2}|p'(0)|, \quad b(x) \geq b_0 > 0. \end{cases} \tag{2.4}$$

In some papers, $x = 0$ is called an attractive turning point because flows on both sides are toward the turning point, and (2.4) is called an attractive turning point problem. Such problems are characterized by the parameter $\lambda = -b(0)/p'(0)$. It is shown [1, 2] that the solution has an interior layer when $\lambda \in (0, 1]$, and the following estimates hold:

$$|u^{(k)}(x)| \le C\big(|x| + \sqrt{\varepsilon}\big)^{\lambda-k}, \quad x \in (-1, 1), \quad k = 0, 1, 2, \dots . \tag{2.5}$$

Similar to the previous case, the first derivative of the solution turns out bounded after multiplying a factor x.

Proposition 2.2. *Suppose u is the solution to (2.4), then there exists a constant C depending on u_L, u_R, f, p, b, which is independent of ε such that*

$$|xu'(x)| \le C, \quad \forall x \in (-1, 1) \tag{2.6}$$

on the assumption that $\lambda \in (0, 1]$.

If $p'(0) > 0$, the problem is also called a repulsive turning point problem, and its solution is smooth near the turning point. Thus we need no additional treatment when dealing with such turning points.

2.3. Boundary turning point problem

Consider the turning point is positioned at an endpoint. We set the interval as $[0, 1]$, and (1.1) becomes

$$\begin{cases} Lu = -\varepsilon u'' + p(x)u' + b(x)u = f(x), & 0 < x < 1, \\ u(0) = u_L, \quad u(1) = u_R, & \\ p(0) = 0, \qquad |p'(x)| \ge \dfrac{1}{2}|p'(0)|, & b(x) \ge b_0 > 0. \end{cases} \tag{2.7}$$

For multiple boundary turning point problems, i.e. $p^{(k)}(0) = 0$ for $k = 1, 2, \dots, m$, it is proved [35] that there exist positive constants C, η depending on u_L, u_R, f, p, b, which are independent of ε such that the following estimates hold:

$$|u^{(k)}(x)| \le C\left(1 + \varepsilon^{-\frac{k}{2}} \exp\left(-\frac{\eta x}{\sqrt{\varepsilon}}\right)\right), \quad x \in (0, 1), \quad k = 0, 1, 2, \dots . \tag{2.8}$$

One can deduce the following result immediately:

$$\begin{aligned} |u^{(k)}(x)| &\le C \min\left\{\big(1 + \varepsilon^{-\frac{k}{2}}\big), (1 + x^{-k})\right\} \\ &= C\big(1 + \big(\max\left\{x, \sqrt{\varepsilon}\right\}\big)^{-k}\big). \end{aligned} \tag{2.9}$$

Now assume that the boundary turning point is single, i.e. $p'(0) \neq 0$. Boundary behaviors of such problems differ from those of (2.1). We introduce the following approximated problem:

$$\begin{cases} \tilde{L}u \equiv -\varepsilon u'' + p'(0)xu' + b(0)u = f(0), & 0 < x < 1, \\ u(0) = u_L, \quad u(1) = u_R, & \\ p'(0) \neq 0, \qquad b(0) > 0. \end{cases} \tag{2.10}$$

We divide the discussion of problem (2.10) into two cases by the sign of $p'(0)$. Inspired by [2], we could represent the solution as a linear combination of Weber's parabolic cylinder functions, which we use to analyze the bounds of the derivatives. The detailed deduction is omitted and the reader could refer to Lemmas A.2 and A.3 in the Appendix A. We only put the main results here that we need in the numerical analysis later.

Proposition 2.3. *For the solution u of (2.7), when $p'(0) > 0$ and $p(1) > 0$, there exists a constant $C = C(u_L, u_R, f, p, b)$ independent of ε, satisfying*

$$|xu'(x)| \le C, \qquad x \le \frac{1}{2}, \tag{2.11a}$$

$$|(1-x)u'(x)| \le C, \quad x \ge \frac{1}{2}. \tag{2.11b}$$

Proposition 2.4. *If u is the solution to (2.7) with $p'(0) < 0$ and $p(1) \le 0$, there exists a constant $C = C(u_L, u_R, f, p, b)$ independent of ε such that*

$$|xu'(x)| \le C. \tag{2.12}$$

3. Numerical Method

In this section, we first introduce some definitions and weak formulations in Section 3.1. We derive the weak solution using a Petrov-Galerkin finite element method (PGFEM), summarized in Algorithm 3.2. If we know the analytic expressions of the solutions to the dual problems, we directly use them as the test functions in PGFEM, otherwise, the dual problems are solved numerically by TFPM on a uniform mesh, as described in Section 3.2. Furthermore, we prove first-order convergency of the approximated operator in L_h^∞-norm and discrete energy norm in Section 3.3. And the nodal values of PGFEM solution are exact when test functions are evaluated exactly (c.f. Theorem 3.3).

3.1. Definitions and formulations

The weak form of problem (1.1) is: Find $u \in H^1(x_L, x_R)$ such that

$$\begin{aligned} &A_\varepsilon(u, v) \equiv \varepsilon(u', v') + (pu', v) + (bu, v) = (f, v), \quad \forall v \in H_0^1(x_L, x_R), \\ &u(x_L) = u_L, \quad u(x_R) = u_R. \end{aligned} \tag{3.1}$$

Let us take a partition $\{x_i, i = 0, 1, \ldots, N\}$ on $[x_L, x_R]$, including any possible interior turning point

$$\begin{aligned} &x_L = x_0 < x_1 < \cdots < x_N = x_R, \\ &I_i = [x_{i-1}, x_i], \qquad i = 1, 2, \ldots, N, \\ &h_i = \begin{cases} x_i - x_{i-1}, & i = 1, \ldots, N, \\ 0, & i = 0, N+1, \end{cases} \end{aligned}$$

and the mesh size h is defined as

$$h = \max_{1 \le i \le N} h_i.$$

In this section, we use L^∞, L^2 and an energy norm $\|\cdot\|_\varepsilon$ for a function u

$$\|u\|_{L^\infty} = \max_{x_L \le x \le x_R} |u(x)|, \tag{3.2}$$

$$\|u\|_{L^2} = \sqrt{\int_{x_L}^{x_R} |u(x)|^2 dx}, \tag{3.3}$$

$$\|u\|_\varepsilon = \sqrt{\|u\|_{L^2}^2 + \varepsilon \|u'\|_{L^2}^2}, \tag{3.4}$$

and the corresponding discrete infinity norm $\|\cdot\|_{L_h^\infty}$ and discrete energy norm $\|\cdot\|_{\varepsilon,h}$ for a grid function u_h

$$\|u_h\|_{L_h^\infty} = \max_{0 \le i \le N} |u_h(x_i)|, \tag{3.5}$$

$$\|u_h\|_{\varepsilon,h} = \sqrt{\|u_h\|_{L_h^2}^2 + \varepsilon \|u_h'\|_{L_h^2}^2}. \tag{3.6}$$

Here L_h^2 is the discrete L^2 space with the norm defined on the grid, and u_h' is computed by a difference scheme

$$\|u_h\|_{L_h^2} = \sqrt{\sum_{i=0}^{N} u_h^2(x_i) \frac{h_i + h_{i+1}}{2}}, \tag{3.7}$$

$$\|u_h'\|_{L_h^2} = \sqrt{\sum_{i=1}^{N} \left(\frac{u_h(x_i) - u_h(x_{i-1})}{h_i} \right)^2 h_i}. \tag{3.8}$$

Before discretization of finite element method, we first approximate (1.1) by the following problem:

$$\begin{cases} \bar{L} u_h \equiv -\varepsilon u_h'' + \bar{p}(x) u_h' + \bar{b}(x) u_h = \bar{f}(x), \quad x_L < x < x_R, \\ u_h(x_L) = u_L, \quad u_h(x_R) = u_R, \end{cases} \tag{3.9}$$

where $\bar{p}, \bar{b}, \bar{f}$ are piecewise approximations to the corresponding functions. Test function space V_h is defined by a group of basis functions $\{\psi_i\}_{i=1}^{N-1}$ with ψ_i solving the dual problem of (3.9) on $I_i \cup I_{i+1}$

$$\begin{cases} \bar{L}^* \psi_i \equiv -\varepsilon \psi_i'' - \bar{p}(x) \psi_i' + \big(\bar{b}(x) - \bar{p}'(x)\big) \psi_i = 0, \quad x_{i-1} < x < x_i, \\ \psi_i(x_{i-1}) = 0, \quad \psi_i(x_i) = 1, \end{cases} \tag{3.10a}$$

$$\begin{cases} \bar{L}^* \psi_i \equiv -\varepsilon \psi_i'' - \bar{p}(x) \psi_i' + \big(\bar{b}(x) - \bar{p}'(x)\big) \psi_i = 0, \quad x_i < x < x_{i+1}, \\ \psi_i(x_i) = 1, \quad \psi_i(x_{i+1}) = 0, \end{cases} \tag{3.10b}$$

$$\operatorname{supp}(\psi_i) = I_i \cup I_{i+1}.$$

Functions $\{\psi_i\}_{i=1}^{N-1}$ are referred to as L^*-splines in some articles.

Then we use PGFEM to discretize the weak form of (3.9): Find $\mathfrak{U}_h \in U_h$ such that

$$\begin{aligned} &\bar{A}_\varepsilon(\mathfrak{U}_h, v_h) \equiv \varepsilon(\mathfrak{U}_h', v_h') + (\bar{p}\mathfrak{U}_h', v_h) + (\bar{b}\mathfrak{U}_h, v_h) = (\bar{f}, v_h), \quad \forall v_h \in V_h, \\ &\mathfrak{U}_h(x_L) = u_L, \quad \mathfrak{U}_h(x_R) = u_R, \end{aligned} \tag{3.11}$$

where

$$U_h = \big\{ v_h \in C[x_L, x_R] \,\big|\, v_h \,|_{\,I_i} \text{ is linear, } i = 1, \dots, N \big\}, \tag{3.12}$$

$$V_h = \left\{ v_h \,\middle|\, v_h = \sum_{i=1}^{N-1} c_i \psi_i, \;\; c_i \in \mathbb{R}, \;\; i = 1, \dots, N-1 \right\}. \tag{3.13}$$

Remark 3.1. If we use parabolic cylinder functions as test functions, it is usual to compute a cut-off of the series expansion of these special functions in order to generate the stiffness matrix and the right-hand-side term. We compute parabolic cylinder functions in MATLAB using codes from Fortran90 by [23,32]. In some cases, numerical cost is expensive when we need these special functions to be precise enough. Moreover, we could not analytically represent the solution to the dual problem with a nonlinear first-order coefficient. In practice, it works as well if we substitute exact evaluations of special functions with numerical solutions described in the following subsection.

3.2. Numerical method of dual problems

We apply TFPM on the uniform mesh to each dual problem. Precisely, for a specific dual problem, we approximate $-\bar{p}(x)$ by a linear function $\hat{a}(x-X_0)$ and $\bar{b}(x)-\bar{p}'(x)$ by a constant $\hat{b}$

$$-\varepsilon\psi'' + \hat{a}(x-X_0)\psi' + \hat{b}\psi = 0, \quad X_1 < x < X_2. \tag{3.14}$$

In practice, we take

$$\begin{aligned}
&\hat{a} = -p'(x^*),\\
&\hat{b} = b(x^*) - p'(x^*),\\
&X_0 = x^* - \frac{p(x^*)}{p'(x^*)},
\end{aligned}$$

where $x^* \in [X_1, X_2]$. The solution ψ is determined with the following boundary conditions:

$$\psi(X_1) = 1, \quad \psi(X_2) = 0. \tag{3.15}$$

We make a uniform partition on the subinterval

$$Y_j = X_1 + j\frac{X_2 - X_1}{N_1}, \quad j = 0, 1, \ldots, N_1.$$

TFPM solution on $[Y_{i-1}, Y_{i+1}]$ is the linear combination of solutions to the equation

$$-\varepsilon\psi'' + \hat{a}(Y_i - X_0)\psi' + \hat{b}\psi = 0, \quad Y_{i-1} < x < Y_{i+1}. \tag{3.16}$$

Eq. (3.16) admits two exponential solutions $\psi^{(1)}, \psi^{(2)}$. Denoting $\psi_i = \psi(Y_i)$, we suppose

$$\alpha_{i,i-1}\psi_{i-1} + \alpha_{i,i}\psi_i + \alpha_{i,i+1}\psi_{i+1} = 0. \tag{3.17}$$

We presume $\alpha_{i,i} = 1$ because (3.16) is homogeneous, and the rest of the coefficients are determined by requiring $\psi^{(1)}$ and $\psi^{(2)}$ to satisfy (3.17)

$$\begin{pmatrix} \psi_{i-1}^{(1)} & \psi_{i+1}^{(1)} \\ \psi_{i-1}^{(2)} & \psi_{i+1}^{(2)} \end{pmatrix} \begin{pmatrix} \alpha_{i,i-1} \\ \alpha_{i,i+1} \end{pmatrix} = - \begin{pmatrix} \psi_i^{(1)} \\ \psi_i^{(2)} \end{pmatrix}. \tag{3.18}$$

By gathering conditions (3.17) at $i = 1, \ldots, N_1 - 1$ together with boundary conditions (3.15), we obtain a tri-diagonal linear system which gives evaluations of approximated dual solutions $\{\psi(Y_i)\}_{i=0}^{N_1}$. We remark that TFPM on the uniform mesh described above yields smaller errors than simple finite difference methods.

To compute derivatives at X_1 and X_2, we represent the solution by exponential basis functions on $[Y_0, Y_1]$ and $[Y_{N_1-1}, Y_{N_1}]$ respectively. For instance, TFPM solution on $[Y_0, Y_1]$ is assumed to satisfy (3.16) which is defined on $Y_0 < x < Y_1$ and Y_i is replaced by $Y_{1/2} = (Y_0 + Y_1)/2$. By boundary conditions at Y_0 and Y_1, the solution is identified on $[Y_0, Y_1]$, and $\psi'(X_1)$ is available by direct calculations.

We summarize the numerical process to solve dual problems in the next algorithm.

Algorithm 3.1: Evaluation of Test Functions ψ and its Derivatives.

1 Specify coefficients $\hat{a}, \hat{b}$, endpoints of the subinterval X_1, X_2 and the boundary condition in the dual equation to be solved, such as (3.14) and (3.15).
2 Make the uniform partition $\{Y_j\}$ on $[X_1, X_2]$.
3 Use the formulation (3.18) to decide the linear relation (3.17) among ψ_{i-1}, ψ_i and ψ_{i+1} for $i = 1, 2, \ldots, N_1 - 1$.
4 Gather the boundary conditions and $N_1 - 1$ relations to form a linear system of $\{\psi_j\}$. Evaluations $\{\psi_j\}$ could be solved.
5 Represent the solution on $[Y_0, Y_1]$ by a linear combination of exponential functions. Then $\psi'(X_1)$ is approximated by the derivative of this combination. Approximation of $\psi'(X_2)$ is similar.

3.3. Main results

We have defined the approximated coefficients and the approximated operator in (3.9). We classify all the subintervals I_k's into ones close to singular points and ones far away. More exactly, we list all singular points in ascending order as $\{s_i\}_{i=1}^{m'}$ which contain any possible interior turning points z_i (with $\lambda_i \in (0, 1]$) and endpoints (with a boundary layer). Let $0 < \delta < \min_i |s_i - s_{i-1}|/3$ and define

$$J_i = [s_i - \delta, s_i + \delta], \quad i = 1, \ldots, m',$$
$$J_r = [x_L, x_R] - \bigcup J_i.$$

According to whether the middle point of a subinterval I_k locates in some J_i or not, we approximate p on I_k by either a linear function or a constant one

$$\bar{p}(x)\big|_{I_k} = \begin{cases} p(x_{k-\frac{1}{2}}), & \text{if} \quad x_{k-\frac{1}{2}} \in J_r, \\ p'(x_k^*)(x - x_k^*) + p(x_k^*), & \text{if} \quad x_{k-\frac{1}{2}} \in J_i, \end{cases}$$

where

$$x_k^* = \begin{cases} s_i, & \text{if} \quad I_k \text{ is adjacent to some } s_i, \\ x_{k-\frac{1}{2}}, & \text{otherwise.} \end{cases}$$

Take $\bar{b}(x)|_{I_k}$ as piecewise constant $b(x_{k-1/2})$ on every subinterval I_k and $\bar{f}(x)|_{I_k}$ likewise. Thus test functions induced by linearly approximated $\bar{p}$ are represented by parabolic cylinder functions and ones derived by constant $\bar{p}$ are exponential functions.

For the difference between L and $\bar{L}$, we have the following theorem.

Theorem 3.1 (First-Order L^∞ Uniform Convergence). *Assume p, b, f as above, and singularities of type* (a), (b), *and* (c) *might occur in the solution. Then the error between*

the solution to (3.9) *and* (1.1) *converges linearly and uniformly in* L^∞ *norm, i.e. there exists a constant* $C = C(u_L, u_R, f, p, b)$ *independent of* h, ε *such that*

$$\|e\|_{L^\infty} \le Ch \tag{3.19}$$

with $e = u - u_h$*, where* u *is the solution to problem* (3.1)*,* u_h *is the solution to problem* (3.9)*.*

Proof. We note that maximum principle holds for L and $\bar{L}$, i.e. there exists a constant $C = C(b_0^{-1})$ independent of ε, h

$$\|v\|_\infty \le C\big(\|Lv\|_\infty + |v(x_L)| + |v(x_R)|\big),$$
$$\|v\|_\infty \le C\big(\|\bar{L}v\|_\infty + |v(x_L)| + |v(x_R)|\big).$$

With the same arguments by Gartland and Farrell [10], we distract the equations of u and u_h and denote $e = u - u_h$

$$\bar{L}e = -(p - \bar{p})u' - (b - \bar{b})u + (f - \bar{f}), \tag{3.20a}$$
$$e(x_L) = e(x_R) = 0. \tag{3.20b}$$

Then from the maximum principle we have

$$\|e\|_\infty \le C\big\{\|(p - \bar{p})u'\|_\infty + \|b - \bar{b}\|_\infty \|u\|_\infty + \|f - \bar{f}\|_\infty\big\}.$$

We separate the discussion of $|e(x)|$ by whether $x_{k-1/2}$ lies in some J_i, where $x \in I_k$.

Case (a) $x_{k-1/2} \in J_i$.

Suppose $x_{k-1/2} \in J_i$. If the singular point $s_i \in (x_L, x_R)$, we have the estimate of the derivative

$$|u'(x)| \le C\big(|x - s_i| + \sqrt{\varepsilon}\big)^{\lambda_i - 1},$$

where the coefficient $\lambda_i = -b(s_i)/p'(s_i) \in (0, 1], |u'(x)|$ is bounded by a constant C for other evaluations of λ. By definition of $\bar{p}$, the term $|(p - \bar{p})u'|$ is under control due to the following inequalities and (2.6):

$$\begin{cases} |p - \bar{p}| \le Ch^2 \le Ch|x - s_i|, & \text{if} \quad |x - s_i| \ge h, \\ |p - \bar{p}| \le C|x - s_i|^2 \le Ch|x - s_i|, & \text{if} \quad |x - s_i| \le h. \end{cases}$$

In both cases $|u'(x)|$ multiplied by $|x - s_i|$ is bounded. The second inequality holds, for we approximate p by the first-order Taylor polynomial at $x = s_i$ in the intervals adjacent to s_i.

In the cases where s_i is an endpoint of the whole interval, generally the derivative $u'(x)$ might be significant near the singular point, such as ε^{-1} or $\varepsilon^{-1/2}$. We have shown in (2.3), (2.11a), and (2.12) that $|(x - s_i)u'(x)|$ is bounded uniformly by a constant C.

Case (b) $x_{k-1/2} \in J_r$.

J_r is δ away from boundary layers and interior layers. Without singularity, we could write the bound of $|u'|$ as C_1, which may depend on a minus power of δ.

In the end, using the facts that $|f - \bar{f}|, |b - \bar{b}| \le Ch$ and $|u| \le C(|f| + |u_L| + |u_R|) \le \tilde{C}$, the first-order convergence in L^∞ norm is proved. □

Now we can discretize the approximated problem (3.11) with the following algorithm.

Algorithm 3.2: PGFEM for Turning Point Problems.

1 Identify singular points s_i and their types of singularities.
2 Take a partition and add in singular points which are absent in the mesh.
3 Approximate p, b, f by piecewise constants or piecewise linear functions based on distance from the midpoint of an interval to singular points (see the definition before Theorem 3.1).
4 Solve dual problems analytically or numerically to evaluate test functions.
5 Generate stiffness matrix and right-hand-side term using test functions.
6 Solve a linear system to obtain the numerical solution $\mathfrak{U}_h$ (on grid points).

Remark 3.2. This algorithm is a fitted operator method because the solution is derived by selecting special test functions, and we need no special mesh on the whole interval. One needs to identify the location of singular points when one constructs the linear system in order to use information of the singularities and to solve dual problems with enough precision.

Theorem 3.2 (First-Order L^2 Uniform Convergence). *Providing the same conditions as the previous theorem, the error between the solution to* (3.9) *and* (1.1) *is linearly and uniformly convergent in L^2-norm and ε-norm, i.e. there exists a constant $C = C(u_L, u_R, f, p, b)$ independent of h and ε such that*

$$\|e\|_{L^2} \le \|e\|_\varepsilon \le Ch. \tag{3.21}$$

Proof. If we consider L^2-norm, we start by (3.20)

$$-\varepsilon e'' + \bar{p}e' + \bar{b}e = F(x) \equiv -(p-\bar{p})u' - (b-\bar{b})u + (f-\bar{f}).$$

We have proved that $|e| \le C|F| \le \tilde{C}h$. On the assumption that $u, u_h \in C^1$, the following energy estimate holds:

$$\int_{x_L}^{x_R} \varepsilon(e')^2 + \left(\bar{b} - \frac{1}{2}\bar{p}'\right) e^2 dx \le \|F\|_{L^2}\|e\|_{L^2} + \frac{1}{2}\sum_{i=1}^{N-1} e^2(x_i)[\bar{p}](x_i). \tag{3.22}$$

For h sufficiently small, using assumption in (1.2), it holds that

$$\bar{b} - \frac{1}{2}\bar{p}' \ge \frac{b_0 + \gamma_0}{4}.$$

Denoting

$$\gamma = \min\left(1, \frac{b_0+\gamma_0}{4}\right),$$

we have the estimate in the energy norm from (3.19) and (3.22)

$$\|e\|_\varepsilon^2 \le Ch^2, \tag{3.23}$$

where the constant C may depend on p, b, f, γ^{-1}, and the jump of $\bar{p}$ is at most Ch

$$\left|[\bar{p}](x_k)\right| \le \left|\bar{p}(x_k^-) - p(x_k)\right| + \left|p(x_k) - \bar{p}(x_k^+)\right| \le Ch.$$

The proof is complete. □

Proposition 3.1 (Numerical Stability). *The scheme satisfies discrete maximum principle, i.e. the matrix induced by PGFEM is tri-diagonally dominated.*

Proof. The stiffness matrix of PGFEM is an M-matrix. It could be verified by taking integrals [10] to (3.10a) and (3.10b). □

We mention that a main feature of our choice of test function space is the zero nodal error. We state this in the next theorem.

Theorem 3.3 (Exactness of Nodal Values). *Assume that we use exact dual solutions as PGFEM test functions, u_h is the solution of* (3.9)*, and $\mathfrak{U}_h$ is the solution of* (3.11)*. Then we have*

$$u_h(x_i) = \mathfrak{U}_h(x_i), \quad \forall i = 0, 1, \ldots, N.$$

Proof. Consider the weak formulations which u_h and $\mathfrak{U}_h$ satisfy

$$\begin{aligned}
&\varepsilon(u_h', v_h') + (\bar{p}u_h', v_h) + (\bar{b}u_h, v_h) = (\bar{f}, v_h), \quad \forall v_h \in H_0^1,\\
&\varepsilon(\mathfrak{U}_h', v_h') + (\bar{p}\mathfrak{U}_h', v_h) + (\bar{b}\mathfrak{U}_h, v_h) = (\bar{f}, v_h), \quad \forall v_h \in V_h.
\end{aligned}$$

We need to assume the regularity of u_h and $\mathfrak{U}_h$ is good enough for further analysis. Denote $E = u_h - \mathfrak{U}_h$ as the error introduced by PGFEM discretization. Take a special test function $v_h = \psi_i$, $i = 1, 2, \ldots, N-1$, and distract the two equation, which gives us

$$\varepsilon(E', \psi_i') + (\bar{p}E' + \bar{b}E, \psi_i) = 0.$$

Integrate by part and substitute in the definition of ψ_i in (3.10a) and (3.10b), then the boundary term remains as follows:

$$\left(\varepsilon E\psi_i' + \bar{p}E\psi_i\right)\big|_{\partial I_i} + \left(\varepsilon E\psi_i' + \bar{p}E\psi_i\right)\big|_{\partial I_{i+1}} = 0.$$

We can check that the coefficient of E_j above is the same with the entry of stiffness matrix when we implement Algorithm 3.2. Assembling $N-1$ such conditions together with $E(x_0)=E(x_N)=0$, we obtain a linear system of $\{E(x_i)\}_{i=0}^N$ which admits only zero solution due to Proposition 3.1. The proof is complete. □

4. Numerical Implementation

In this section, we use three examples to validate the efficiency and convergency of our algorithm. Different cases of singularities (a), (b), and (c) are included in these examples. Test functions could be computed with exact parabolic cylinder functions or approximated by numerical solutions. PGFEM solutions with fine girds ($N = 4096$) using exact test functions are chosen to be reference solutions in the first two examples; the third one admits an exact solution. We calculate errors by $\|\cdot\|_{L_h^\infty}$, $\|\cdot\|_{L_h^2}$ and $\|\cdot\|_{\varepsilon,h}$ defined in (3.5)-(3.8).

Example 4.1. Consider a turning point problem with a cusp-like interior layer and an exponential-type boundary layer

$$\begin{cases}
-\varepsilon u'' + \cos(2\pi x)u' + u = \dfrac{1}{1+x^2}, \quad 0 < x < 1,\\
u(0) = 1, \quad u(1) = 2.
\end{cases}$$

There is an interior layer at $x = 1/4$ and a boundary layer at $x = 1$, corresponding to cases (b) and (a). We set $\{1/4, 3/4, 1\}$ to be singular points which need special care. Although the condition (1.2) for $(b - p')$ is not satisfied in this case, while numerical experiments indicate that Algorithm 3.2 still works if properly treated. If we take $\bar{p}$ as piecewise linear function in a δ-neighborhood of the repulsive turning point $x = 3/4$, we use the exact solution of the dual problem as test functions; if we take $\bar{p}$ as piecewise constant function, we could use the exact solution or the approximate solution of the dual problem as test functions. In practice we take δ in Theorem 3.1 as follows in all three examples:

$$\delta = \min\left\{0.1,\ \frac{\min_i |s_i - s_{i-1}|}{3}\right\},$$

where s_i are all the singular points.

The reference solution, together with numerical solutions using PGFEM on the uniform mesh and an up-winding scheme on Shishkin mesh [22] with both 256 grids are shown in Fig. 4.1. Exact dual solutions are selected as test functions. Compared to non-equidistant mesh of Shishkin type, PGFEM needs no special grids, and values on the uniform mesh points are highly accurate. The solution using Shishkin mesh has a lower resolution outside the interior layer, which could be improved by mesh refinement. PGFEM errors in three different discrete norms versus grid number N are drawn with a log-log plot in Fig. 4.2, where one may find a nearly second-order convergency.

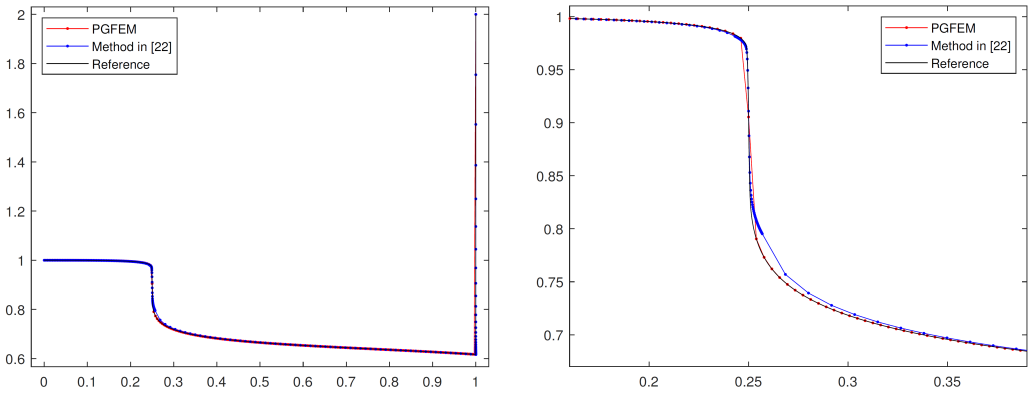

(a) (b)

Fig. 4.1. Numerical and reference solutions for Example 4.1 ($\varepsilon = 1 \times 10^{-6}$), where test functions in PGFEM are calculated with exact expressions. (a) PGFEM and the method in [22] are employed with grid number $N = 256$, with the latter using an up-winding scheme on Shishkin mesh. The reference solution is computed with PGFEM on grids $N = 4096$, (b) Horizontal magnification near $x = 1/4$.

Remark 4.1. As we evaluate all the coefficients at the middle points of intervals, we could even observe the second-order convergency from the numerical results.

Example 4.2. Consider a boundary turning point problem

$$\begin{cases} -\varepsilon u'' + (1 - x^2)u' + 3u = e^x, & -1 < x < 1, \\ u(-1) = 1, \quad u(1) = 2. \end{cases}$$

At both endpoints the solution appears singular with $p'(-1) > 0$ at $x = -1$ and $p'(1) < 0$ at $x = 1$, corresponding to case (c) with a positive slope and a negative one. These two boundary layers are weaker than those in Example 4.1, as the PGFEM solution and the reference solution are drawn in Fig. 4.3. Setting $\{-1, 1\}$ as singular points and exact dual solutions as test functions, L_h^∞ errors and discrete energy errors are shown in Tables 4.1 and 4.2 accordingly, where a second-order uniform convergence could be verified.

For Example 4.2, if we compute test functions numerically, using the same reference solution, convergence is the same as above (see Table 4.3). Convergency also holds for multiple turning point problems if we follow the same procedure to compute test functions, although it is unclear what analytic expressions of the solutions to dual problems are.

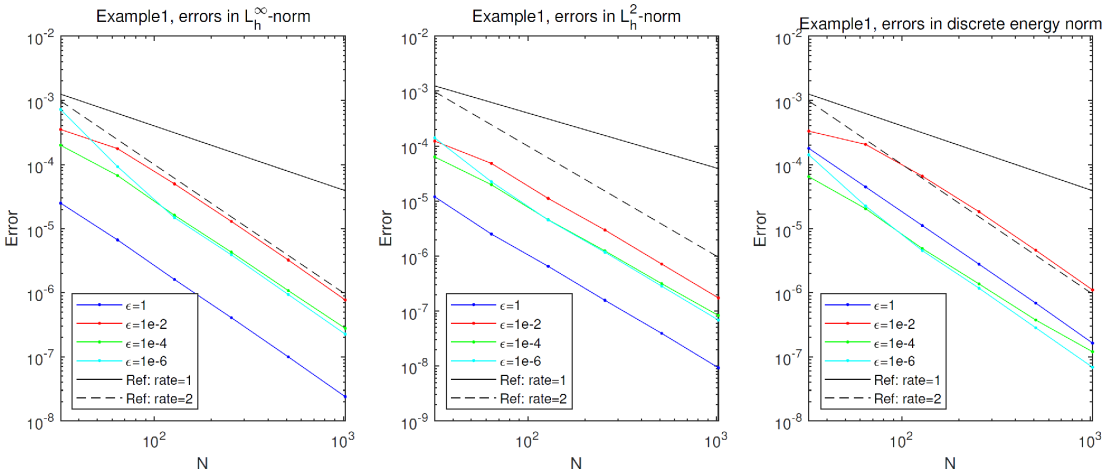

Fig. 4.2. Log-log plot for PGFEM errors in Example 4.1 versus grid number N, in L_h^∞, L_h^2 and discrete energy norm. The solid black line and black dashed line have slopes -1 and -2, respectively.

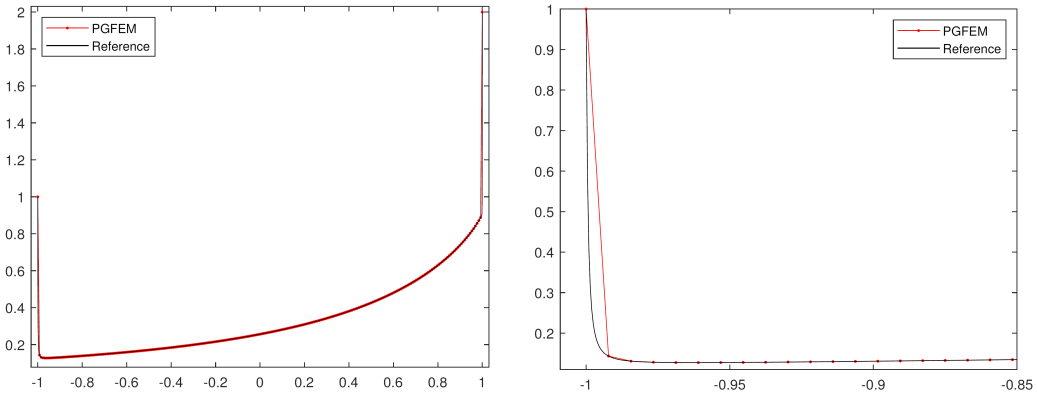

(a) (b)

Fig. 4.3. Numerical and reference solutions for Example 4.2 ($\varepsilon = 1 \times 10^{-6}$). Test functions in PGFEM are calculated with exact expressions. (a) PGFEM is implemented with grids $N = 256$, and the reference solution is calculated using the same algorithm with $N = 4096$, (b) Horizontal magnification near $x = 0$.

Table 4.1: L_h^∞ errors of PGFEM solutions for Example 4.2. Test functions are calculated with exact expressions.

ε	1		1E-02		1E-04		1E-06	
N	L_h^∞	Rate	L_h^∞	Rate	L_h^∞	Rate	L_h^∞	Rate
32	1.12E-04		2.78E-03		1.85E-03		1.85E-03	
64	2.39E-05	2.43	1.46E-03	1.52	7.22E-04	2.10	7.16E-04	1.93
128	5.97E-06	2.00	3.72E-04	1.97	1.90E-04	1.93	1.83E-04	1.97
256	1.56E-06	1.98	7.86E-05	2.37	4.49E-05	2.26	8.66E-05	2.31
512	3.85E-07	2.02	1.94E-05	2.01	1.41E-05	1.89	3.73E-05	2.45
1024	9.07E-08	2.10	4.83E-06	2.04	3.33E-06	2.08	1.51E-05	2.22

Table 4.2: $\|\cdot\|_{\varepsilon,h}$ errors of PGFEM solutions for Example 4.2. Test functions are calculated with exact expressions.

ε	1		1.E-02		1.E-04		1.E-06	
N	Energy	Rate	Energy	Rate	Energy	Rate	Energy	Rate
32	3.93E-04		1.95E-03		6.38E-04		6.27E-04	
64	9.56E-05	2.24	9.93E-04	1.52	2.08E-04	1.84	2.09E-04	1.77
128	2.39E-05	2.00	2.55E-04	1.97	5.31E-05	1.99	5.50E-05	2.01
256	6.02E-06	2.03	5.47E-05	2.37	1.51E-05	2.17	1.42E-05	2.18
512	1.49E-06	2.02	1.35E-05	2.01	4.46E-06	2.01	3.93E-06	2.15
1024	3.53E-07	2.08	3.36E-06	2.05	1.24E-06	2.03	1.14E-06	2.13

Table 4.3: L_h^∞ errors of PGFEM solutions for Example 4.2. Test functions are approximated by numerical solutions.

ε	1		1.E-02		1.E-04		1.E-06	
N	L_h^∞	Rate	L_h^∞	Rate	L_h^∞	Rate	L_h^∞	Rate
32	1.12E-04		2.78E-03		1.86E-03		1.86E-03	
64	2.39E-05	2.43	1.46E-03	1.52	7.23E-04	2.11	7.21E-04	1.94
128	5.96E-06	2.00	3.72E-04	1.97	1.90E-04	1.93	1.84E-04	1.97
256	1.56E-06	1.98	7.86E-05	2.37	4.50E-05	2.26	8.66E-05	2.32
512	3.85E-07	2.02	1.94E-05	2.01	1.40E-05	1.89	3.68E-05	2.45
1024	9.07E-08	2.10	4.83E-06	2.04	3.33E-06	2.08	1.51E-05	2.29

Example 4.3. Consider the following multiple boundary turning point problem [35]:

$$\begin{cases} -\varepsilon u'' - x^3 u' + u = f(x), \quad 0 < x < 1, \\ u(0) = 2, \quad u(1) = e^{-\frac{1}{\sqrt{\varepsilon}}} + e, \end{cases}$$

where $f(x)$ is determined by the exact solution

$$u(x) = e^{-\frac{x}{\sqrt{\varepsilon}}} + e^x.$$

There is a $\sqrt{\varepsilon}$-wide boundary layer at the turning point $x = 0$, as drawn in Fig. 4.4.

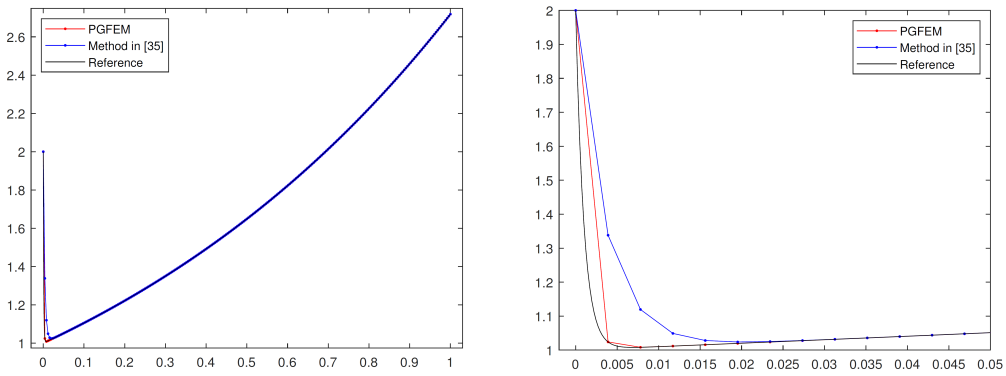

(a) (b)

Fig. 4.4. Numerical and exact solutions for Example 4.3 ($\varepsilon = 1 \times 10^{-6}$). Test functions in PGFEM are approximated by numerical solutions on grids $N_1 = 4096$. (a) PGFEM and the method in [35] are manipulated with uniform grids $N = 256$, and the reference solution is computed with PGFEM and $N = 4096$, (b) Horizontal magnification near $x = 0$.

Results of PGFEM are compared with one in [35], where we compute with two methods on the same uniform mesh, and PGFEM obtains solutions with higher precision. In this case, analytic expressions of dual solutions are unknown. Thus we utilize numerical solutions to dual problems as test functions. The L_h^∞ convergence rate of PGFEM is almost two, as shown in Table 4.4.

Table 4.4: L_h^∞ errors of PGFEM solutions for Example 4.3. Test functions are approximated by numerical solutions.

ε	1		1.E-02		1.E-04		1.E-06	
N	L_h^∞	Rate	L_h^∞	Rate	L_h^∞	Rate	L_h^∞	Rate
32	1.84E-05		1.65E-04		3.71E-04		1.05E-03	
64	4.61E-06	2.00	4.82E-05	1.77	5.89E-05	2.66	3.01E-04	1.81
128	1.15E-06	2.00	1.26E-05	1.93	8.85E-06	2.82	7.64E-05	1.98
256	2.88E-07	2.00	3.20E-06	1.98	2.22E-06	1.99	1.77E-05	2.11
512	7.21E-08	2.00	8.02E-07	2.00	5.50E-07	2.01	4.57E-06	2.31
1024	1.79E-08	2.01	2.01E-07	2.00	1.33E-07	2.04	1.17E-06	1.97

5. Conclusion

In this paper, we develop a Petrov-Galerkin finite element method (PGFEM) to solve a class of turning point problems in one dimension. A priori estimates have been established for the single boundary turning point case. Numerical analysis shows that our scheme has first-order uniform convergency in several different discrete norms. In numerical examples, errors in different discrete norms validate the feasibility and efficiency of the scheme. We emphasize that such an algorithm not only could be implemented with evaluations of exact solutions to the dual problems but also is considerable if test functions are approximated numerically.

Appendix A. A Priori Estimates for Single Boundary Turning Point Problems

A.1. Preparations for estimates

We introduce a lemma to estimate the solution u more precisely.

Lemma A.1. *There exists one and only one solution u to (2.7). Besides, there is a constant $C = C(u_L, u_R, f, p, b)$ independent with ε such that*

$$|p(x)u'(x)| \le C, \quad \forall x \in [0, 1/2]. \tag{A.1}$$

Proof. We suffice to show that $\varepsilon u''(x)$ is bounded by C on $[0, 1/2]$, for u could be bounded by f using the maximum principle. First assume that $p'(0) = -\alpha < 0$, and let $z(x) = u''(x)$. Differentiate (2.7) once, and we have

$$-\varepsilon z' + p(x)z = s(x),$$

where

$$\begin{aligned} s(x) &= s_1(x) + s_2(x), \\ s_1(x) &= f'(x) - b'(x)u, \\ s_2(x) &= -\big(p'(x) + b(x)\big)u'. \end{aligned}$$

Let $P(x) = -\int_0^x p(t)dt$. Since $p'(x) \le -\alpha/2 < 0$, after some basic calculus we have

$$\begin{aligned} -\frac{P(x)}{\varepsilon} &\le 0, \\ P(t) - P(x) &= \int_t^x p(\tau)d\tau \le 0 \end{aligned}$$

for $0 < t < x$. By variance of constants we have

$$z(x) = z(0)\exp\left(-\frac{P(x)}{\varepsilon}\right) - \varepsilon^{-1}\int_0^x \exp\left(\frac{P(t) - P(x)}{\varepsilon}\right) s(t)dt. \tag{A.2}$$

Taking $x = 0$ in (2.7),

$$z(0) = \varepsilon^{-1}\big(b(0)u(0) - f(0)\big) = C\varepsilon^{-1}.$$

The integral in the second term of (A.2) is split into terms with s_1 and s_2

$$\begin{aligned} I_1 &= \int_0^x \exp\left(\frac{P(t) - P(x)}{\varepsilon}\right) s_1(t)dt \le \int_0^x 1 \cdot Cdt = C, \\ I_2 &= \int_0^x \exp\left(\frac{P(t) - P(x)}{\varepsilon}\right) s_2(t)dt \le C, \end{aligned}$$

where we use the second mean value theorem for integrals for the second inequality. Thus we have shown that $\varepsilon u''(x)$ is bounded on $[0, 1]$ if $p'(0) < 0$.

In the case $p'(0) = \alpha > 0$, the same argument could be repeated with the following modification:

$$z(x) = \exp\left(\frac{P(1/2) - P(x)}{\varepsilon}\right) z\left(\frac{1}{2}\right) - \varepsilon^{-1}\int_x^{\frac{1}{2}} \exp\left(\frac{P(\tau) - P(x)}{\varepsilon}\right) s(\tau)d\tau,$$

where $|z(1/2)|$ is bounded by C. The result here applies only for $x \in [0, 1/2]$ because (2.7) may have a boundary layer at $x = 1$. □

We have shown that $p(x)u'(x)$ is bounded near the singular point $x = 0$. The original problem (2.7) is solved by decomposing $u = u_1 + u_2 + u_0$

$$\begin{aligned} &u_0 = \frac{f(0)}{b(0)}, \\ &\begin{cases} \tilde{L}u_1 = 0, & 0 < x < 1, \\ u_1(0) = u_L - u_0, \quad u_1(1) = u_R - u_0, \end{cases} \\ &\begin{cases} \tilde{L}u_2 = g(x), \quad 0 < x < 1, \\ u_2(0) = u_2(1) = 0, \end{cases} \end{aligned} \tag{A.3}$$

where $\tilde{L}$ is defined in (2.10), and

$$g(x) \equiv \big(f(x) - f(0)\big) - \big(p(x) - p'(0)x\big)u' - \big(b(x) - b(0)\big)u.$$

From Lemma A.1 we could write

$$g(x) = h(x)x,$$

where $|h(x)|$ is bounded by a constant depending on p, b and f for $x \in [0, 1/2]$. We solve u_1 by direct representation with parabolic cylinder functions, while u_2 is related to Green's function for $\tilde{L}$.

A.2. Basic property of parabolic cylinder function

Parabolic cylinder functions $U(a, x), V(a, x)$, using Weber's notations, are linear independent solutions to the equation

$$-y'' + \left(a + \frac{x^2}{4}\right) y = 0,$$

where a is a coefficient. The following properties will be used later [23, 32]:

$$\pi V(a,x) = \Gamma\left(\frac{1}{2} + a\right)\big(\sin \pi a \cdot U(a,x) + U(a,-x)\big), \tag{A.4a}$$

$$\Gamma\left(\frac{1}{2} + a\right) U(a,x) = \pi \sec^2 \pi a \big(V(a,-x) - \sin \pi a \cdot V(a,x)\big), \tag{A.4b}$$

$$\sqrt{2\pi} U(a,ix) = \Gamma\left(\frac{1}{2} - a\right)\left(e^{-i\pi(-\frac{a}{2}-\frac{1}{4})} U(-a,x) + e^{i\pi(-\frac{a}{2}-\frac{1}{4})} U(-a,-x)\right), \tag{A.4c}$$

$$U'(a,x) + \frac{1}{2}xU(a,x) + \left(a + \frac{1}{2}\right) U(a+1,x) = 0, \tag{A.4d}$$

$$U'(a,x) - \frac{1}{2}xU(a,x) + U(a-1,x) = 0, \tag{A.4e}$$

$$V'(a,x) + \frac{1}{2}xV(a,x) - V(a+1,x) = 0, \tag{A.4f}$$

$$V'(a,x) - \frac{1}{2}xV(a,x) - \left(a - \frac{1}{2}\right) V(a-1,x) = 0, \tag{A.4g}$$

$$U(a,x) = \exp\left(-\frac{1}{4}x^2\right) x^{-a-\frac{1}{2}} \delta_1, \quad x \geq C_0, \tag{A.4h}$$

$$V(a,x)=\sqrt{\frac{2}{\pi}}\exp\left(\frac{1}{4}x^2\right)x^{a-\frac{1}{2}}\delta_2,\quad x\geq C_0. \tag{A.4i}$$

$C_0=\mathcal{O}(1)$ is a constant related to a, and coefficients δ_1,δ_2 satisfy

$$|\delta_i-1|\leq\frac{1}{3}.$$

A.3. Green's function of the operator $\tilde{L}$

Denote μ_0 by the solution to

$$\begin{cases}\tilde{L}u=0,\\ u(0)=0,\quad u(1)=1,\end{cases}$$

and μ_1 by the solution to

$$\begin{cases}\tilde{L}u=0,\\ u(0)=1,\quad u(1)=0.\end{cases}$$

The Wronskian of μ_0 and μ_1 is

$$W(x)=W(\mu_0,\mu_1)=\mu_0(x)\mu_1'(x)-\mu_1(x)\mu_0'(x).$$

The Green's function of $\tilde{L}$ is piecewise defined on $[0,1]$

$$G(x,\tau)=\begin{cases}-\varepsilon^{-1}\mu_0(x)\mu_1(\tau)\dfrac{\exp\left((p'(0)/2\varepsilon)(1-\tau^2)\right)}{W(1)},&0\leq x\leq\tau\leq 1,\\ -\varepsilon^{-1}\mu_1(x)\mu_0(\tau)\dfrac{\exp\left((p'(0)/2\varepsilon)(1-\tau^2)\right)}{W(1)},&0\leq\tau\leq x\leq 1,\end{cases}$$

which satisfies

$$\begin{aligned}&\tilde{L}G(x,\tau)=\delta(x-\tau),\\ &G(0)=G(1)=0.\end{aligned}$$

u_2 defined in (A.3) could be represented as

$$u_2(x)=\int_0^1 G(x,\tau)\tau h(\tau)d\tau.$$

Thus estimates for u_2 turn into ones for $G(\cdot,\tau)$ and its derivatives.

A.4. The case $p'(0)=\alpha>0$

We first estimate derivatives of the solution u in the next lemma.

Lemma A.2. *Assume u is the solution to (2.7) with $p'(0)>0$, and $\rho=C_0\sqrt{\varepsilon}$, where C_0 is defined in Section A.2. For $k=1,2,\ldots,$*

$$\left|u^{(k)}(x)\right|\leq\begin{cases}C(1+\rho^{-k}),&0\leq x\leq\rho,\\ C(1+x^{-k}),&\rho\leq x\leq\dfrac{1}{2},\end{cases} \tag{A.5}$$

where C depends on u_L,u_R,f,p,b. Rewriting these estimates in a more compact form, we have

$$\left|u^{(k)}(x)\right|\leq C\big(1+(\max\{x,\rho\})^{-k}\big),\quad 0\leq x\leq\frac{1}{2}. \tag{A.6}$$

Proof. Since u_0 in (A.3) has no contribution to the derivative, for the sake of simplicity, we replace u by $u_1 + u_2$ and still denote it by u. We introduce the following change of variable, for both u_1 and u_2 satisfy an equation of $\tilde{L}$:

$$\tilde{x} = \frac{x}{\sqrt{\varepsilon/\alpha}},$$
$$u_1(x) = \tilde{u}(\tilde{x}) \exp\left(\frac{\tilde{x}^2}{4}\right).$$

Denoting $\beta = b(0)/\alpha > 0$, we obtain the equation for $\tilde{u}$

$$-\tilde{u}'' + \left(\frac{\tilde{x}^2}{4} + \beta - \frac{1}{2}\right)\tilde{u} = 0.$$

$\tilde{u}$ admits linear independent solutions $U(\beta - 1/2, \tilde{x}), V(\beta - 1/2, \tilde{x})$. Hence,

$$u_1(x) = c_1 \exp\left(\frac{\tilde{x}^2}{4}\right) U\left(\beta - \frac{1}{2}, \tilde{x}\right) + c_2 \exp\left(\frac{\tilde{x}^2}{4}\right) V\left(\beta - \frac{1}{2}, \tilde{x}\right).$$

Coefficients c_1, c_2 are determined by boundary conditions

$$\begin{pmatrix} U\left(\beta - \frac{1}{2}, 0\right) & V\left(\beta - \frac{1}{2}, 0\right) \\ \exp\left(\frac{\alpha}{4\varepsilon}\right) U\left(\beta - \frac{1}{2}, \frac{1}{\sqrt{\varepsilon/\alpha}}\right) & \exp\left(\frac{\alpha}{4\varepsilon}\right) V\left(\beta - \frac{1}{2}, \frac{1}{\sqrt{\varepsilon/\alpha}}\right) \end{pmatrix} \begin{pmatrix} c_1 \\ c_2 \end{pmatrix} = \begin{pmatrix} u_L \\ u_R \end{pmatrix}.$$

Call the matrix on the left-hand side A. Denoting K_i as constants of $\mathcal{O}(1)$, we could rewrite A in the asymptotic form

$$A \approx \begin{pmatrix} K_1 & K_2 \\ K_3 \varepsilon^{\frac{\beta}{2}} & K_4 \exp\left(\frac{\alpha}{2\varepsilon}\right) \varepsilon^{\frac{1-\beta}{2}} \end{pmatrix}.$$

Therefore the coefficients are represented as follows:

$$\begin{pmatrix} c_1 \\ c_2 \end{pmatrix} = A^{-1} \begin{pmatrix} u_L \\ u_R \end{pmatrix}.$$

We omit all the constants of $\mathcal{O}(1)$ for simplicity. Considering $u_L, u_R = \mathcal{O}(1)$, the derivatives are in the following form:

$$\begin{aligned} {u_1}^{(k)}(x) &= \varepsilon^{-\frac{k}{2}} \left[c_1 \exp\left(\frac{\tilde{x}^2}{4}\right) \Pi_{i=1}^{k} (-\beta - i + 1) U\left(\beta + k - \frac{1}{2}, \tilde{x}\right) + c_2 \exp\left(\frac{\tilde{x}^2}{4}\right) V\left(\beta + k - \frac{1}{2}, \tilde{x}\right) \right] \\ &= \varepsilon^{-\frac{k}{2}} \left[c_1' \exp\left(\frac{\tilde{x}^2}{4}\right) U\left(\beta + k - \frac{1}{2}, \tilde{x}\right) + c_2 \exp\left(\frac{\tilde{x}^2}{4}\right) V\left(\beta + k - \frac{1}{2}, \tilde{x}\right) \right]. \end{aligned}$$

For convenience, write $u_1(x) = u_L \mu_1(x) + u_R \mu_0(x)$, and we estimate μ_0 and μ_1 first in order to estimate u_1 and its derivatives on $[0, 1/2]$

$$\left|\mu_0^{(k)}(x)\right| \le \begin{cases} C \exp\left(-\frac{\alpha}{2\varepsilon}\right) \varepsilon^{\frac{\beta - k - 1}{2}}, & |x| \le \rho, \\ C\left(\exp\left(-\frac{\alpha}{2\varepsilon}\right) \varepsilon^{\beta - \frac{1}{2}} x^{-\beta - k} + \varepsilon^{-k} \exp\left(-\frac{\alpha}{2\varepsilon}(1 - x^2)\right) x^{\beta + k - 1}\right), & \rho \le |x| \le 1, \end{cases}$$

$$\left|\mu_1^{(k)}(x)\right| \le \begin{cases} C\varepsilon^{-\frac{k}{2}}, & |x| \le \rho, \\ C\left(\varepsilon^{\frac{\beta}{2}} x^{-\beta - k} + \exp\left(-\frac{\alpha}{2\varepsilon}(1 - x^2)\right) \varepsilon^{\frac{\beta}{2} - k} x^{\beta + k - 1}\right), & \rho \le |x| \le 1, \end{cases}$$

which hold for $k = 0, 1, 2, \dots$. Thus

$$|W(1)| \geq C\varepsilon^{\frac{\beta}{2}-1}.$$

If $x \leq \rho$, from

$$u_1^{(k)} = u_L\mu_1^{(k)} + u_R\mu_0^{(k)},$$

we have

$$\begin{aligned}\left|u_1^{(k)}(x)\right| &\leq C\Big(|u_R|\left|\mu_0^{(k)}(x)\right| + |u_L|\left|\mu_1^{(k)}(x)\right|\Big)\\ &\leq C\left(|u_R|\exp\left(-\frac{\alpha}{2\varepsilon}\right)\varepsilon^{\frac{\beta-k-1}{2}} + |u_L|\varepsilon^{-\frac{k}{2}}\right)\\ &\leq C\rho^{-k}, \quad k = 1, 2, \dots .\end{aligned}$$

If $\rho \leq x \leq 1/2$,

$$\exp\left(-\frac{\alpha}{2\varepsilon}(1-x^2)\right) \leq \exp\left(-\frac{\alpha'}{2\varepsilon}\right),$$

where $\alpha' = 3\alpha/4$, we have

$$\begin{aligned}\left|u_1^{(k)}(x)\right| &\leq C|u_L|\left(\varepsilon^{\frac{\beta}{2}}x^{-\beta-k} + \exp\left(-\frac{\alpha}{2\varepsilon}(1-x^2)\right)\varepsilon^{\frac{\beta}{2}-k}x^{\beta+k-1}\right)\\ &\quad + C|u_R|\left(\exp\left(-\frac{\alpha}{2\varepsilon}\right)\varepsilon^{\beta-\frac{1}{2}}x^{-\beta-k} + \varepsilon^{-k}\exp\left(-\frac{\alpha}{2\varepsilon}(1-x^2)\right)x^{\beta+k-1}\right)\\ &\leq C(1+x^{-k}), \quad k = 1, 2, \dots .\end{aligned}$$

Constant C may depend on β, k, α, C_0. Derivatives of u_2 are estimated by induction

$$\begin{aligned}\left|u_2'(x)\right| &\leq C\int_0^1 |G_x(x,\tau)|\tau d\tau\\ &= \begin{cases}\displaystyle\int_0^x + \int_x^\rho + \int_\rho^1, & 0 \leq x \leq \rho,\\ \displaystyle\int_0^\rho + \int_\rho^x + \int_x^1, & \rho \leq x \leq \frac{1}{2}.\end{cases}\end{aligned}$$

After some standard computation, we could verify the first derivative of u_2 satisfies (A.5) with $k = 1$.

We have to obtain estimates for $u_1^{(k)}$ and u_2' in the same form. Considering that the behavior near $x = 1$ has been studied well as an exponential boundary layer, we narrow down the a priori estimate for u to $[0, 1/2]$

$$|u'(x)| \leq \begin{cases}C(1+\rho^{-1}), & 0 \leq x \leq \rho,\\ C(1+x^{-1}), & \rho \leq x \leq \dfrac{1}{2}.\end{cases}$$

For higher derivatives $u^{(k)} (k \geq 2)$, we could differentiate $(k-1)$ times the equation in (2.7) and split $v = u^{(k-1)}$ into three parts as u is decomposed in (A.3). It is noticed that v satisfies a similar equation to (2.10), with β replaced by $\beta+k-1$ and boundary conditions in asymptotic forms. Actually, we can obtain by induction, for $k = 1, 2, \dots,$

$$\begin{aligned}u^{(k)}(0) &= \varepsilon^{-\frac{k}{2}},\\ u^{(k)}(1) &= \varepsilon^{-k}.\end{aligned}$$

Simple calculations yield the following result:

$$|u^{(k)}(x)| \le \begin{cases} C(1+\rho^{-k}), & 0 \le x \le \rho, \\ C(1+x^{-k}), & \rho \le x \le \dfrac{1}{2}. \end{cases}$$

The proof is complete. □

Remark A.1. If we take $x \approx 1$ into consideration, the estimates could be modified as

$$|u^{(k)}(x)| \le \begin{cases} C(1+\rho^{-k}), & 0 \le x \le \rho, \\ C\Big(1+x^{-k}+(1-x)^{-k}\Big), & \rho \le x \le 1, \end{cases} \quad k = 1, 2, \dots . \tag{A.7}$$

Note that for $1/2 \le x \le 1$,

$$\exp\left(-\frac{\alpha}{2\varepsilon}(1-x^2)\right) \le C\left(\frac{\varepsilon}{1-x}\right)^k.$$

The following proposition holds as a direct conclusion, and we will use these propositions to show the convergence of the numerical method.

A.5. The case $p'(0) = -\alpha < 0$

In this case, estimates for derivatives of u are mildly different.

Lemma A.3. *Assume that u is the solution to (2.7) when $p'(0) < 0$ and $p(1) < 0$. Let $\beta = b(0)/\alpha > 0$, and ρ is defined as above. Then we have the following estimates:*

$$|u^{(k)}(x)| \le \begin{cases} C(1+\rho^{\beta-k}+|u_L|\rho^{-k}), & 0 \le x \le \rho, \\ C(1+x^{\beta-k}+|u_L|x^{-k}), & \rho \le x \le 1, \end{cases} \quad k = 1, 2, \dots, \tag{A.8}$$

where C depends on u_L, u_R, f, p, b. Or otherwise in a compact form

$$|u^{(k)}(x)| \le C\big(1+(\max\{x,\rho\})^{\beta-k}+|u_L|(\max\{x,\rho\})^{-k}\big), \quad 0 \le x \le 1, \quad k = 1, 2, \dots . \tag{A.9}$$

Proof. If we let $\tilde{x} = x/\sqrt{-\varepsilon/\alpha}$, the new variable becomes pure imaginary. From the property that evaluation of $U(a, iz)$ and $V(a, iz)$ could be represented by $U(-a, z), V(-a, z)$ (c.f. (A.4a),(A.4c)), we assume the solution to be

$$u(x) = c_1 \exp\left(\frac{\tilde{x}^2}{4}\right) U\left(\frac{1}{2}+\beta, |\tilde{x}|\right) + c_2 \exp\left(\frac{\tilde{x}^2}{4}\right) V\left(\frac{1}{2}+\beta, |\tilde{x}|\right).$$

For simplicity we denote $\hat{x} = |\tilde{x}| = x/\sqrt{\varepsilon/\alpha}$, which gives

$$u(x) = c_1 \exp\left(-\frac{\hat{x}^2}{4}\right) U\left(\frac{1}{2}+\beta, \hat{x}\right) + c_2 \exp\left(-\frac{\hat{x}^2}{4}\right) V\left(\frac{1}{2}+\beta, \hat{x}\right).$$

Again we solve coefficients c_1, c_2 from boundary conditions u_L, u_R. Let

$$A = \begin{pmatrix} U\left(\dfrac{1}{2}+\beta, 0\right) & V\left(\dfrac{1}{2}+\beta, 0\right) \\ \exp\left(-\dfrac{\alpha}{4\varepsilon}\right) U\left(\dfrac{1}{2}+\beta, \dfrac{1}{\sqrt{\varepsilon/\alpha}}\right) & \exp\left(-\dfrac{\alpha}{4\varepsilon}\right) V\left(\dfrac{1}{2}+\beta, \dfrac{1}{\sqrt{\varepsilon/\alpha}}\right) \end{pmatrix}$$

$$\approx \begin{pmatrix} K_1 & K_2 \\ K_3 \exp\left(-\frac{\alpha}{2\varepsilon}\right) \varepsilon^{\frac{1+\beta}{2}} & K_4 \varepsilon^{-\frac{\beta}{2}} \end{pmatrix}.$$

Then c_1, c_2 could be written as

$$\begin{pmatrix} c_1 \\ c_2 \end{pmatrix} = A^{-1} \begin{pmatrix} u_L \\ u_R \end{pmatrix}.$$

As the previous case, for $k = 1, 2, \ldots,$

$$u^{(k)}(x) = \varepsilon^{-\frac{k}{2}} \left[c_1' \exp\left(-\frac{\hat{x}^2}{4}\right) U\left(\beta + \frac{1}{2} - k, \hat{x}\right) + c_2' \exp\left(-\frac{\hat{x}^2}{4}\right) V\left(\beta + \frac{1}{2} - k, \hat{x}\right) \right].$$

For $\mu_0, \mu_1,$ and $k = 0, 1, 2, \ldots,$

$$\mu_0^{(k)}(x) = \exp\left(-\frac{\hat{x}^2}{4}\right) \varepsilon^{\frac{\beta-k}{2}} \left(U\left(\beta + \frac{1}{2} - k, \hat{x}\right) + V\left(\beta + \frac{1}{2} - k, \hat{x}\right) \right),$$
$$\mu_1^{(k)}(x) = \exp\left(-\frac{\hat{x}^2}{4}\right) \varepsilon^{-\frac{k}{2}} \left(U\left(\beta + \frac{1}{2} - k, \hat{x}\right) + \varepsilon^{\frac{1}{2}+\beta} \exp\left(-\frac{\alpha}{2\varepsilon}\right) V\left(\beta + \frac{1}{2} - k, \hat{x}\right) \right).$$

We have the following estimates:

$$\left|\mu_0^{(k)}(x)\right| \leq \begin{cases} C\varepsilon^{\frac{\beta-k}{2}}, & x \leq \rho, \\ C\left(\exp\left(-\frac{\alpha}{2\varepsilon}x^2\right) \varepsilon^{\beta+\frac{1}{2}-k} x^{-\beta+k-1} + x^{\beta-k}\right), & x \geq \rho, \end{cases}$$
$$\left|\mu_1^{(k)}(x)\right| \leq \begin{cases} C\varepsilon^{-\frac{k}{2}}, & x \leq \rho, \\ C\left(\exp\left(-\frac{\alpha}{2\varepsilon}x^2\right) \varepsilon^{\frac{\beta+1}{2}-k} x^{-\beta+k-1} + \exp\left(-\frac{\alpha}{2\varepsilon}\right) \varepsilon^{\frac{\beta+1}{2}} x^{\beta-k}\right), & x \geq \rho, \end{cases} \quad k = 0, 1, \ldots.$$

Since these two estimates are different from the case $p'(0) > 0$, we might keep u_L and u_R as independent variables

$$\begin{aligned} \left|u_1^{(k)}(x)\right| &\leq |u_R| \left|\mu_0^{(k)}(x)\right| + |u_L| \left|\mu_1^{(k)}(x)\right| \\ &\leq \begin{cases} C\left(|u_R|\varepsilon^{\frac{\beta-k}{2}} + |u_L|\varepsilon^{-\frac{k}{2}}\right), & x \leq \rho, \\ C\left(|u_R|x^{\beta-k} + |u_L|x^{-k}\right), & x \geq \rho, \end{cases} \quad k = 1, 2, \ldots. \end{aligned}$$

u_2 could be estimated similarly by computing integrals of Green's function. We omit these details and present the following result:

$$\left|u_2^{(k)}(x)\right| \leq \begin{cases} C(1 + \rho^{\beta-k}), & x \leq \rho, \\ C(1 + x^{\beta-k}), & x \geq \rho, \end{cases} \quad k = 1, 2, \ldots.$$

The conclusion in Lemma A.3 consists of estimates for u_1 and u_2. □

Remark A.2. The solution of the case $p'(0) < 0$ is smooth at the endpoint $x = 1$, hence, estimates are made on the whole interval $[0, 1]$. The result in Lemma A.3 is quite similar to [2], except that nonzero u_L might lower the regularity of the solution.

Remark A.3. Estimates (2.8) are stronger than Lemmas A.2 and A.3. Analysis in [35] applies in the cases $k \geq 2$, where k stands for multiples of the turning point, while the same argument

no longer holds for $k = 1$. Another difference is that their estimates are made on the whole interval $[0, 1]$. In contrast, estimates hold for $[0, 1/2]$ in Lemma A.2 and for the whole interval in Lemma A.3. Estimates (A.5) and (A.8) give upper bounds for $x \leq \rho$ and $x \geq \rho$ separately when the turning point is single, and it is unknown whether these estimates could be combined into one expression in an essential way.

Acknowledgments. This work was partially supported by the NSFC (Grant No. 12025104).

References

[1] L.R. Abrahamson, A priori estimates for solutions of singular perturbations with a turning point, *Stud. Appl. Math.*, **56**:1 (1977), 51–69.

[2] A.E. Berger, H. Han, and R.B. Kellogg, A priori estimates and analysis of a numerical method for a turning point problem, *Math. Comput.*, **42**:166 (1984), 465–492.

[3] D. Broersen and R. Stevenson, A robust Petrov-Galerkin discretisation of convection-diffusion equations, *Comput. Math. Appl.*, **68**:11 (2014), 1605–1618.

[4] A. Chakraborty, A. Rangarajan, and G. May, Optimal approximation spaces for discontinuous Petrov-Galerkin finite element methods, *arXiv:2012.12751*, 2020.

[5] L. Chen, Y. Wang, and J. Wu, Stability of a streamline diffusion finite element method for turning point problems, *J. Comput. Appl. Math.*, **220**:1-2 (2008), 712–724.

[6] C. De Falco and E. O'Riordan, A parameter robust Petrov-Galerkin scheme for advection-diffusion-reaction equations, *Numer. Algorithms*, **56**:1 (2011), 107–127.

[7] P.P.N. De Groen and P.W. Hemker, Error bounds for exponentially fitted Galerkin methods applied to stiff two-point boundary value problems, in: *Numerical Analysis of Singular Perturbation Problems*, Academic Press, (1979), 217–249.

[8] T.M. El-Mistikawy and M.J. Werle, Numerical method for boundary layers with blowing – The exponential box scheme, *AIAA J.*, **16**:7 (1978), 749–751.

[9] P.A. Farrell, Sufficient conditions for the uniform convergence of a difference scheme for a singularly perturbed turning point problem, *SIAM J. Numer. Anal.*, **25**:3 (1988), 618–643.

[10] P.A. Farrell and E.C. Gartland, Jr., A uniform convergence result for a turning point problem, in: *Proc. BAIL V Conference*, (1988), 127–132.

[11] F.Z. Geng, S.P. Qian, and S. Li, A numerical method for singularly perturbed turning point problems with an interior layer, *J. Comput. Appl. Math.*, **255** (2014), 97–105.

[12] W. Guo, *Uniformly Convergent Finite Element Methods for Singularly Perturbed Parabolic Partial Differential Equations*, PhD Thesis, University College Cork, 1993.

[13] H. Han and Z. Huang, Tailored finite point method for steady-state reaction-diffusion equations, *Commun. Math. Sci.*, **8**:4 (2010), 887–899.

[14] H. Han and Z. Huang, Tailored finite point method based on exponential bases for convection-diffusion-reaction equation, *Math. Comput.*, **82**:281 (2013), 213–226.

[15] H. Han, Z. Huang, and R.B. Kellogg, A tailored finite point method for a singular perturbation problem on an unbounded domain, *J. Sci. Comput.*, **36**:2 (2008), 243–261.

[16] P.W. Hemker, G.I. Shishkin, and L.P. Shishkina, ε-uniform schemes with high-order time-accuracy for parabolic singular perturbation problems, *IMA J. Numer. Anal.*, **20**:1 (2000), 99–121.

[17] Z. Huang, Tailored finite point method for the interface problem, *Netw. Heterog. Media*, **4**:1 (2009), 91–106.

[18] R.B. Kellogg and A. Tsan, Analysis of some difference approximations for a singular perturbation problem without turning points, *Math. Comput.*, **32**:144 (1978), 1025–1039.

[19] D. Kumar, A parameter-uniform method for singularly perturbed turning point problems exhibiting interior or twin boundary layers, *Int. J. Comput. Math.*, **96**:5 (2019), 865–882.

[20] J. Li, Convergence analysis of finite element methods for singularly perturbed problems, *Comput. Math. Appl.*, **40**:6–7 (2000), 735–745.

[21] J.B. Munyakazi, K.C. Patidar, and M.T. Sayi, A robust fitted operator finite difference method for singularly perturbed problems whose solution has an interior layer, *Math. Comput. Simulation*, **160** (2019), 155–167.

[22] S. Natesan, J. Jayakumar, and J. Vigo-Aguiar, Parameter uniform numerical method for singularly perturbed turning point problems exhibiting boundary layers, *J. Comput. Appl. Math.*, **158**:1 (2003), 121–134.

[23] F.W.J. Olver, D.W. Lozier, R.F. Boisvert, and C.W. Clark, *NIST Handbook of Mathematical Functions Hardback and CD-ROM*, Cambridge University Press, 2010.

[24] R.E. O'Malley, Jr., On boundary value problems for a singularly perturbed differential equation with a turning point, *SIAM J. Math. Anal.*, **1**:4 (1970), 479–490.

[25] E. O'Riordan and J. Quinn, Parameter-uniform numerical methods for some linear and nonlinear singularly perturbed convection diffusion boundary turning point problems, *BIT Numer. Math.*, **51**:2 (2011), 317–337.

[26] E. O'Riordan and J. Quinn, A singularly perturbed convection diffusion turning point problem with an interior layer, *Comput. Methods Appl. Math.*, **12**:2 (2012), 206–220.

[27] H.-G. Roos, Global uniformly convergent schemes for a singularly perturbed boundary-value problem using patched base spline-functions, *J. Comput. Appl. Math.*, **29**:1 (1990), 69–77.

[28] M. Stynes and E. O'Riordan, A finite element method for a singularly perturbed boundary value problem, *Numer. Math.*, **50**:1 (1986), 1–15.

[29] M. Stynes and E. O'Riordan, L^1 and L^∞ uniform convergence of a difference scheme for a semilinear singular perturbation problem, *Numer. Math.*, **50**:5 (1987), 519–531.

[30] G. Sun and M. Stynes, Finite element methods on piecewise equidistant meshes for interior turning point problems, *Numer. Algorithms*, **8**:1 (1994), 111–129.

[31] G. Sun and M. Stynes, Finite-element methods for singularly perturbed high-order elliptic two-point boundary value problems. I: Reaction-diffusion-type problems, *IMA J. Numer. Anal.*, **15**:1 (1995), 117–139.

[32] N.M. Temme, Numerical and asymptotic aspects of parabolic cylinder functions, *J. Comput. Appl. Math.*, **121**:1–2 (2000), 221–246.

[33] R. Vulanović, Non-equidistant generalizations of the Gushchin-Shchennikov scheme, *ZAMM Z. Angew. Math. Mech.*, **67**:12 (1987), 625–632.

[34] R. Vulanović, On numerical solution of a mildly nonlinear turning point problem, *Esaim Math. Model. Numer. Anal.*, **24**:6 (1990), 765–783.

[35] R. Vulanović and P.A. Farrell, Continuous and numerical analysis of a multiple boundary turning point problem, *SIAM J. Numer. Anal.*, **30**:5 (1993), 1400–1418.

[36] S. Yadav and P. Rai, An almost second order hybrid scheme for the numerical solution of singularly perturbed parabolic turning point problem with interior layer, *Math. Comput. Simulation*, **185** (2021), 733–753.